

Article

Prototype of an Ankle Neurorehabilitation System with Heuristic BCI Using Simplified Fuzzy Reasoning

Norihiko Saga *, Yasuto Tanaka, Atsushi Doi, Teruo Oda, Suguru N. Kudoh and Hiroyuki Fujie

Department of Human System Interaction, School of Science and Technology, Kwansei Gakuin University, Gakuen, Sanda 669-1337, Japan; yasutotanaka2016@gmail.com (Y.T.); ehk97596@kwansei.ac.jp (A.D.); teruo.oda.kwansei@gmail.com (T.O.); snkudoh@kwansei.ac.jp (S.N.K.); hiroyuki.fujie@paris-miki.jp (H.F.)

* Correspondence: saga@kwansei.ac.jp; Tel.: +81-79-565-7042

Received: 28 April 2019; Accepted: 6 June 2019; Published: 14 June 2019



Abstract: Neurorehabilitation using a brain–computer interface (BCI) requires machine learning, for which calculations take a long time, even days. However, the demands of actual rehabilitation are becoming increasingly rigorous, requiring that processes be completed within tens of minutes. Therefore, we developed a new effective rehabilitation system for treating patients such as those with stroke hemiplegia. The system can smoothly perform rehabilitation training on the day of admission to the hospital. We designed a heuristic BCI with simplified fuzzy reasoning, which can detect motor intention signals from an electroencephalogram (EEG) within several tens of minutes. The detected signal is sent to the newly developed ankle rehabilitation device (ARD), and the patient repeats the dorsiflexion motion by the ARD.

Keywords: ankle rehabilitation; brain–computer interface (BCI); EEG; fuzzy template matching; neurorehabilitation

1. Introduction

As of 2016, Japan’s elderly population, people older than 65 years old, was 34.61 million, accounting for 27.3% of the whole population [1]. This report underscores the severity of Japan’s rapidly aging society. According to Ministry of Health, Labor, and Welfare statistics, the primary reason for care nursing is stroke, which accounts for 21.5% of all cases requiring care [2]. Cerebral stroke causes intellectual disability and language disorders, together with hemiplegia of every body part including the legs. Early rehabilitation is necessary to treat hemiplegia. Training to improve range of motion and muscle strength is typically conducted using a continuous passive motion (CPM) device [3,4]. However, such efforts are ineffective after the chronic phase more than six months after cerebral infarction.

Among the promising techniques is a brain–computer interface (BCI) by which electroencephalogram (EEG) signals (i.e., surface electrical brain activity measured on multiple electrodes placed on the scalp) are typically used to operate the rehabilitation device. Such a device provides visual stimulation that evokes brain activity of event-related potentials (ERP) [5,6] or steady-state visually evoked potentials (SSVEP), which correspond to the temporal frequency of the stimulus [7,8].

One field for BCI application is physical rehabilitation. Recently, so-called repetitive facilitative exercise (Kawahira method) [9,10] has drawn attention in the rehabilitation field. Stimulation is given to the neural system (brain) by observing an affected limb with motor intention (imagery), while the therapist moves the limb. This stimulation can be applied to injured muscles or tendons. Such treatment might facilitate the development of a novel neural circuit responsible for intentional movement by reconstructing novel circuitry and improving motor ability. This “neurorehabilitation” is expected to be beneficial for patients with chronic difficulties.

A fundamental human behavior is walking, and the ability to walk supports the independent life of an elderly person. Thus, ankle joint rehabilitation is emphasized, because it is indispensable in forming a prosperous and vigorous society with elderly people living longer, maintaining and improving their activities of daily life (ADLs) and quality of life (QOL) and maintaining their ability to walk independently. Rehabilitation related to the ankle is of interest because (1) although several studies have addressed lower limb issues such as ankle control and improvement [4,11], fewer studies have examined BCI, except as related to the upper limbs; and (2) generally speaking, gait is a universal behavior involving the ankle, which is an important structure supporting body weight. Consequently, constructing ankle rehabilitation devices is a crucially important issue related to BCI.

For actual rehabilitation purposes, the time allocated to feature extraction should be short, possibly with completion in hours. Existing learning algorithms [5–8] usually take several weeks to months for machine learning calculations to extract characteristic EEG patterns from a specific frequency range.

Therefore, the goal of this study is to construct a neurorehabilitation system to extract motor intentions rapidly. We developed two methods: (1) heuristic BCI using fuzzy template matching (FTM), because the process quickly and simply extracts characteristic EEG patterns, and (2) ankle rehabilitation devices (ARDs) that change the load automatically according to the degree of contracture. Two elements constitute the ankle neurorehabilitation system (ANS).

This report describes the development of an ANS prototype: (1) an overview of the heuristic BCI system, (2) design and control of the ARD, and (3) an overview of the entire system comprising these two components. Finally, we present results of actual experiments conducted while operating the system.

2. Heuristic BCI Using L-FTM

In this chapter, we describe fuzzy template matching based on simplified fuzzy reasoning, which detects motion intention from measured EEG signals.

2.1. Measurement of EEG Signal

We used a portable, multichannel, biopotential measurement system (Active Two, Biosemi, Amsterdam, Netherlands) to record the EEG signals. A participant wears a head cap, with Ag-AgCl active electrodes connected to an amplifier with which EEG signals from the brain are measured from the scalp. The head cap with 16-pin active electrodes was set according to the standard international 10–20 system. The reference common-mode-sense (CMS) electrode and the driven-right-leg (DRL) electrode were located in the parietal region. The task was to use imagery of the right ankle at 30° dorsiflexion. The EEG signals during the task and during a resting period were detected, then sent to the amplifier, where they were A/D converted and sent through a USB receiver (via optic fiber) to a PC, where data were processed using LabVIEW 2015 software (National Instruments Corp., Austin, TX, USA). The sampling frequency was 2048 Hz. For signal processing, fast Fourier transform (FFT) was applied to the EEG signal detected from each electrode. The sum of the power values in the range of the selected frequency band was obtained and used as the input value. For the two frequency bands selected as input, we used α -band (8–13 Hz) and β -band (14–50 Hz); this is a wider range definition than the conventional one.

2.2. Heuristic BCI Using L-FTM

The heuristic BCI we developed for detection of motor intention uses learning-type fuzzy template matching (L-FTM) [12] based on simplified fuzzy reasoning. The flow of the heuristic BCI process is presented in Figure 1.

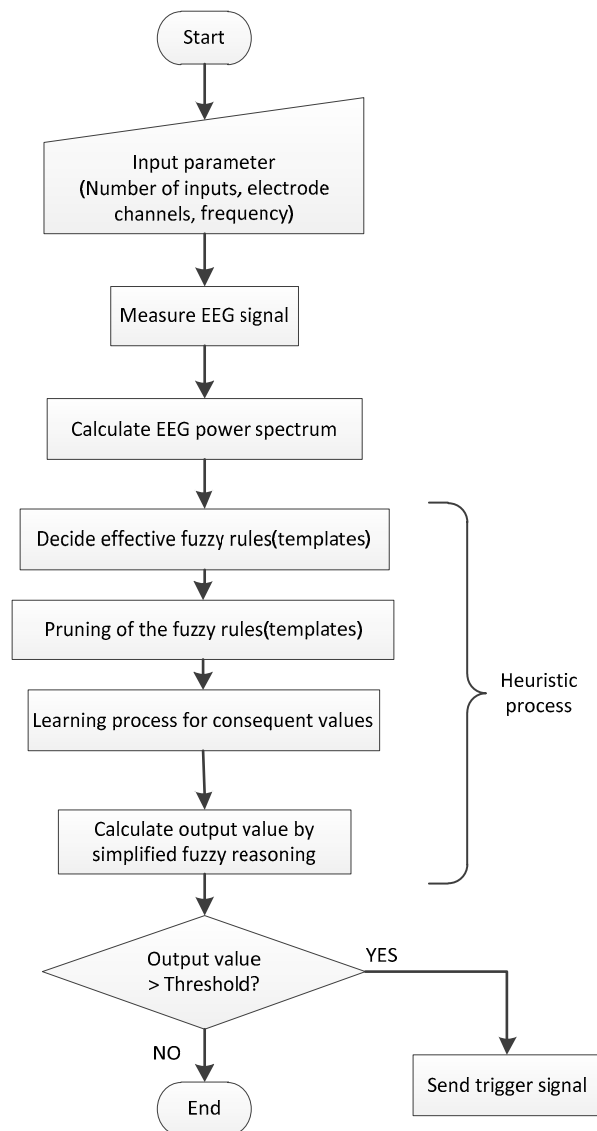


Figure 1. Block diagram of heuristic brain–computer interface (BCI) system. Electroencephalogram (EEG).

2.2.1. Fuzzy Template Matching (FTM)

This study uses FTM [12], a method of template matching based on simplified fuzzy reasoning. Each fuzzy template was constructed with two fuzzy labels of “high” and “low” in an antecedent clause of a fuzzy rule. As shown in Figure 2, the 2^{16} rule is constructed from 16 inputs based on the number of EEG measurement channels (8 electrodes, 2 frequencies), and 2 inputs based on the number of fuzzy labels. For instance, a template can be composed of inputs having features of different types such as “EEG power of Oz measurement site in the α wave frequency band” and “amplitude of the surface electromyography (EMG) signal of the lower right limb.” This approach, which reduces the computational complexity of the heuristic BCI, can classify EEG signals quickly into several categories linked respectively to specific cognitive states.

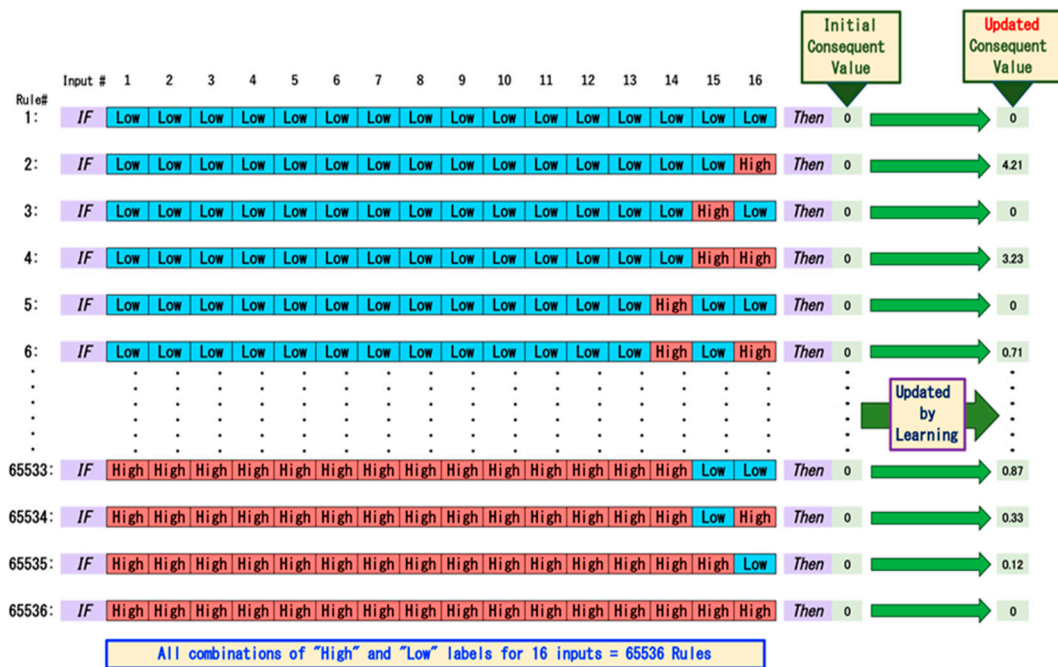


Figure 2. Learning of fuzzy template matching (FTM) system.

Each membership function in a rule (template) is constructed by calculating the power of each channel (microV2) and finding maximum and minimum values. The domain of membership function was ascertained from the maximum and minimum values of the power. The shape of the membership function is a symmetrical triangle, where the peak turns to 1 located at the middle of the domain and the bottom turns to zero [13,14].

The EEG power was input to the membership function of the defined fuzzy label of the j th input of the i th fuzzy rule. The multiplied outputs of all membership functions of the i th fuzzy rule, G_j , are obtained as the compatibility degree of the i th fuzzy rule, μ_i , which is expressed as Equation (1):

$$\mu_i = \prod_{j=0}^n G_j \tag{1}$$

Output value Z was calculated as the weighted average of the consequent values of all rules. Here, Z_i is the consequent value of the i th rule, which is described as Equation (2):

$$Z = \frac{\sum_{i=1}^n (\mu \cdot Z_i)}{\sum_{i=1}^n \mu_i} \tag{2}$$

The output value corresponds to the relative compatibility degree during motor imagery.

2.2.2. Pruning Fuzzy Rules

Fuzzy rule sets were automatically generated from EEG feature patterns from combinations of input and fuzzy labels such as "high" and "low." Rules with a high degree of compatibility for the EEG during both "task" and "nontask" status were expected to be included. Such fuzzy rules compatible with both states reduce the identification accuracy. To avoid this adverse effect, we implemented "pruning" [15].

The pruning process deletes inadequate fuzzy rules with a high degree of compatibility for both states. We retained only rules with a high degree of compatibility for either a task state or a nontask

state. The maximum value of the compatibility degree of the i th fuzzy rule during the task situation was calculated as $Ob_{(i)}$, which is described as Equation (3):

$$Ob_{(i)} = \max \left\{ \sum_{t=1}^{te} Ot_{(i,t)}, \sum_{t=1}^{te} On_{(i,t)} \right\} \tag{3}$$

where t is the time of input data, te is the last time, and $O_{t(i,t)}$ and $O_{n(i,t)}$ are the degree of compatibility of the i th rule at time t during the task and nontask status, respectively. Then, the difference between the total value of each degree of compatibility is calculated. Its absolute value is $O_{s(i)}$, as presented in Equation (4):

$$O_{s(i)} = \left| \sum O_{t(i)} - \sum O_{n(i)} \right| \tag{4}$$

If the value of $O_{s(i)}$ normalized with $O_{s(i)}$ is lower than the adequately set threshold, then the i th rule is judged to have a high degree of compatibility in both states and is deleted. If the difference is large, then the i th rule is judged to have a high degree of compatibility only for task or nontask status. The rule was retained as shown in Equation (5):

$$Pruning(R_{(i)}) = \begin{cases} \text{retain, if } \left(\frac{Ob_{(i)}}{O_{s(i)}} \geq th \right) \\ \text{delete, if } \left(\frac{O_{s(i)}}{Ob_{(i)}} < th \right) \end{cases} \tag{5}$$

Using only retained subsets of templates (rules), the learning process was undertaken with input values of those stored for pruning. The consequent values of the subset of rules (templates) were set by learning processes. The new template set increases the accuracy of identification of the two states, as shown in Figure 3.

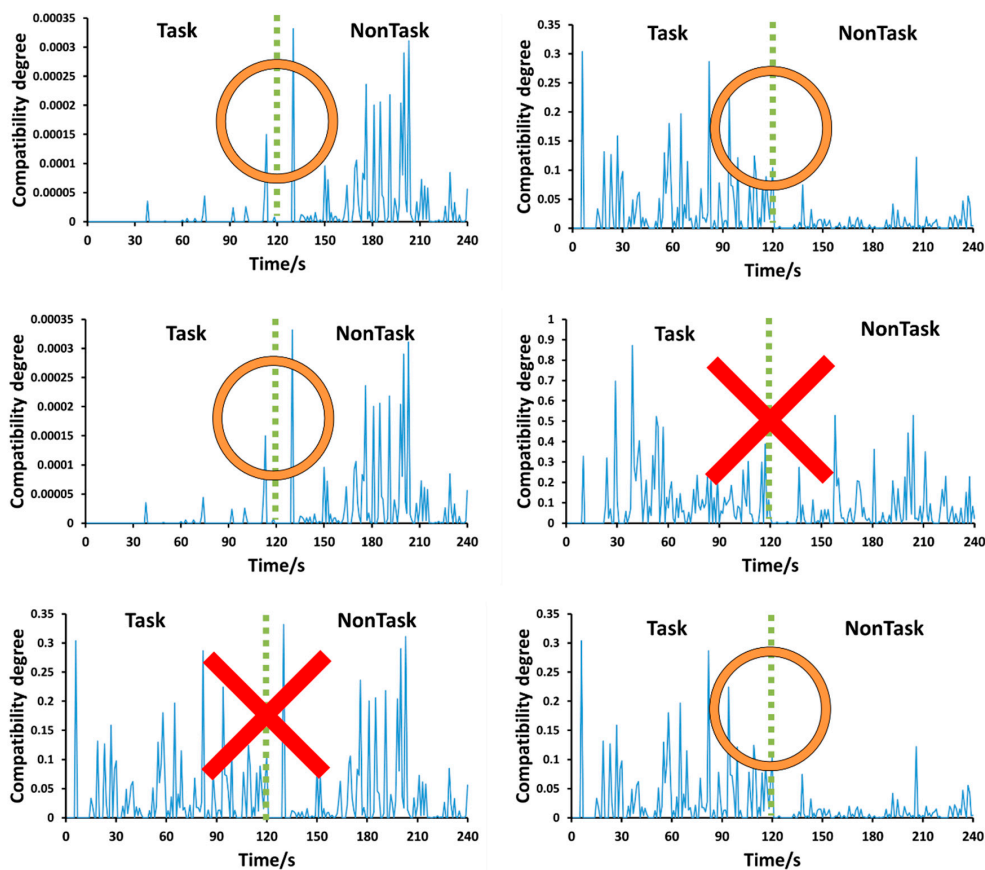


Figure 3. Results of the pruning process.

Consequent values were set up by the learning process [15,16]. Using the steepest descent method, Z is approximated to the target value of the teacher signal T in Equation (6). Z'_i is the consequent value before updating, which differs from Z_i . Here, ρ is a learning coefficient, as shown below:

$$Z_i = Z'_i + \rho \cdot \mu_i \cdot (T - Z). \quad (6)$$

The teacher signal is allowed to be any value if the values can be linked to several distinct states. Initially, 0 was set as the resting state of the EEG and five as a label for the EEG during foot movement. In the learning process, consequent values of rules with a high degree of compatibility for a certain state are modified to the teacher signal corresponding to the state, thereby producing effective rules (templates) for recognition of the specific status. Recognized EEG features during a cognitive task are then extracted from the rule set consisting of the combination of labels (a sort of searching process).

The output signal is binary sorted through a thresholding function. The threshold is set according to the level of the power of the task and the resting state (Figure 10). When the output value of FTM surpasses the threshold, a trigger is generated, which is transmitted to the ankle rehabilitation device (ARD).

3. Ankle Rehabilitation Device (ARD)

3.1. Mechanical Design

In this section, details of the ARD are described [17,18]. The ARD consists of a pneumatic cylinder, a footrest for placing one's feet, a stopper part that physically suppresses excessive bottom dorsiflexion exceeding the set angle of the footrest, a calf placement holder, and a frame that supports all the parts, as shown in Figure 4.

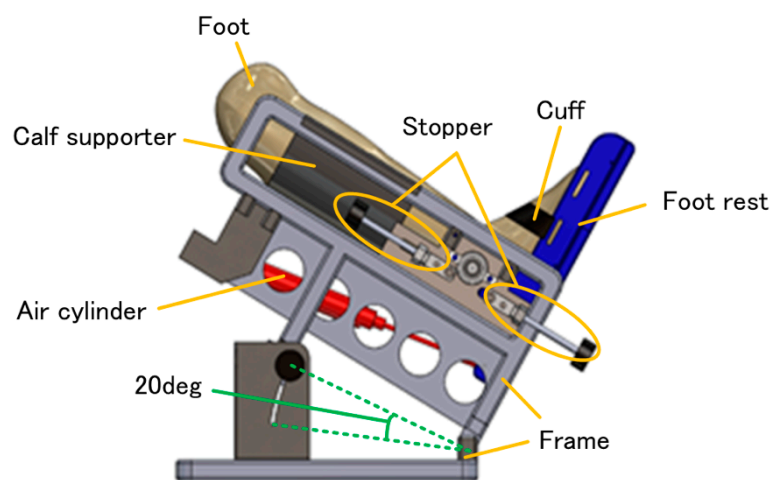


Figure 4. Ankle rehabilitation device (ARD).

The general CPM is the motor drive. Compared to the motor, the pneumatic actuator is lightweight, with high shock absorption. Therefore, this highly portable ARD is unlikely to hurt a user. The angle adjuster portrayed in the figure can be rotated 65°. The structure was designed for use even in a recumbent or seated position. During the rehabilitation operation, the cylinder's straight motion is switched to rotational motion in the ankle position, producing the mechanism shown in Figure 5, which trains up to 20° of dorsiflexion and 45° of plantar flexion. The range of angle motion was designed according to the actual ankle joint range of motion defined by the Japan Rehabilitation Medical Society.

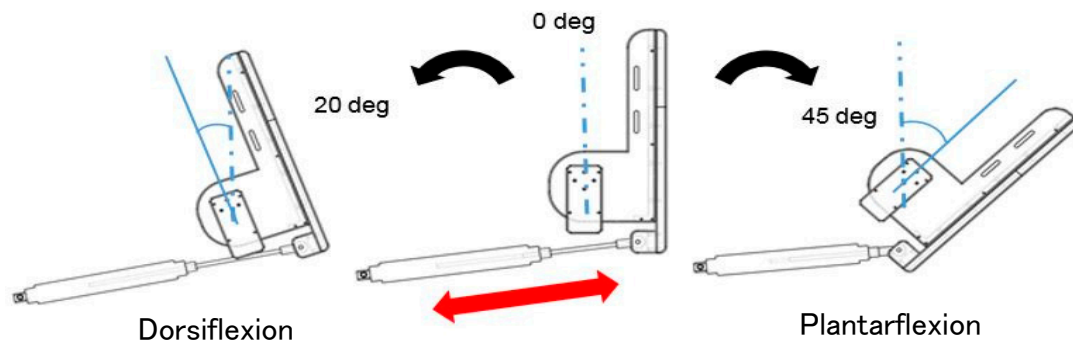
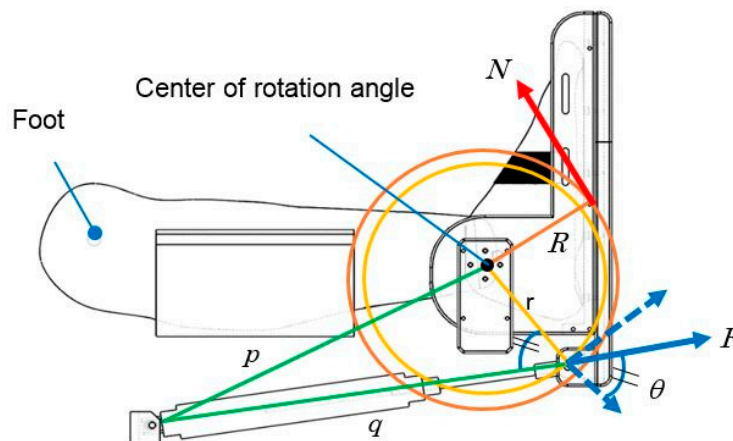


Figure 5. Ankle joint range of motion.

3.2. Pneumatic Cylinder Selection

We chose a pneumatic cylinder that satisfies the required stroke and thrust from the geometric relationship between the cylinder and the footrest. The required specification is a stroke with angles of -20° to $+45^\circ$, as described above, and a force of 40 N, which is the average force of a woman’s hand pressing on the sole of the foot [19]. We investigated and compared calculated values and actual measurements, which is the relationship between the ankle joint angle, the thrust, and the force applied to the sole of the foot. Here, R , r , and p remain invariable even when the footrest rotates, as shown in Figure 6.



N , foot reaction force; F , cylinder thrust; q , cylinder length; θ , angle between q and r ; R , distance from axis of rotation of footrest to measurement position; r , distance from axis of rotation of footrest to attachment part of cylinder rod and footrest from rotation axis of footrest; p , distance from cylinder mounting part to rotation axis.

Figure 6. Parameters for calculation of foot reaction force.

We next present formulas for calculating θ from the cosine theorem and for obtaining foot reaction force N by moment balancing, as Equations (7) and (8), respectively:

$$\cos\theta = \frac{q^2 + r^2 - p^2}{2qr} \tag{7}$$

$$N = \frac{F \sin\theta \cdot r}{R} \tag{8}$$

Calculations based on these equations revealed that strokes require the total 141.8 mm of -43.6 mm in the pushing direction and 98.2 mm in the pulling direction, considering the range of the footrest angle (-20° to $+45^\circ$). The cylinder thrust can be obtained by: (pressure receiving area) \times (internal cylinder pressure). Originally, a reciprocating cylinder should have been chosen. However, because this study covers ankle contracture in patients with cerebral infarction, portability must be achieved through size and weight reduction. The angle must be considered all in dorsiflexion directions, because this research assumes a pointy foot based on the patient’s ankle joint contracture. For that reason, a single-acting cylinder was chosen for dorsiflexion operation.

The thrust of the selected pneumatic cylinder (M24D 150.0 Airpel, Airpot Corp. Norwalk, CT, USA) was a theoretical (calculated) value of 40 N; thrust of 40.1 N was confirmed in the experimentally obtained result. The stroke was more than 141.8 mm and the thrust was stronger than 40 N, both satisfying the necessary specifications.

3.3. Control System Design

To replicate the rehabilitation operation of a physical therapist, the ankle rehabilitation device was designed with a control system to switch from position control to force control. With this position control, training for the target angle is repeated for a healthy person or a user with weak contracture of the ankle. If the position control is performed by contracture, it is switched to force control for patients who do not reach the target angle. A flowchart is shown in Figure 7.

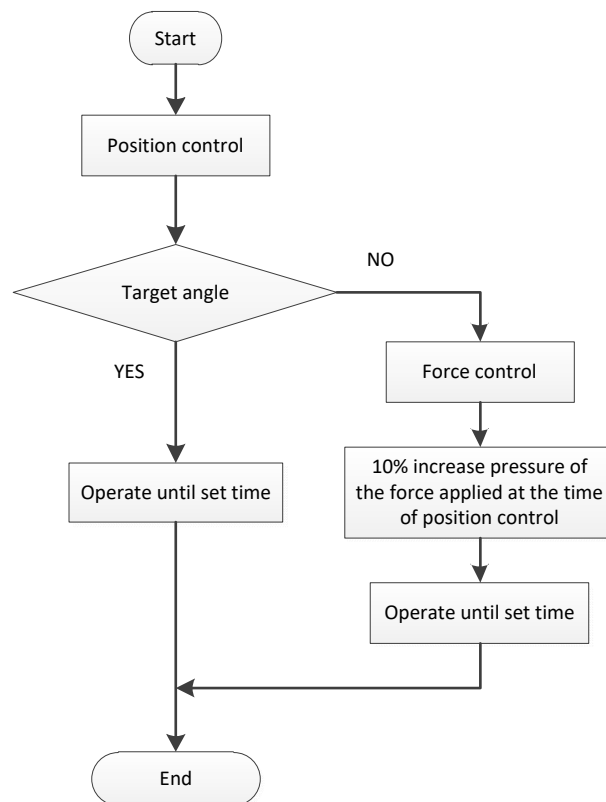


Figure 7. Flowchart of switching control from position control to force control.

When the program begins, position control is used to reach the target angle, then continues as it is. If the target angle is reached, it is maintained for the set time. The device is set to switch to force control unless it reaches the target angle even after 5 s have elapsed. Under force control, a 10% addition of the force applied under position control is exerted, which imitates the physical therapist’s action of adding a little force when the ankle becomes stuck. The rehabilitation system realizes both position control and force control by proportional-integral-derivative (PID) control. Therefore, we performed a control

experiment to ascertain the parameters of P, I, and D and verify the switching control. We restricted the angle using the stopper on the ankle rehabilitation device and reproduced the situation where it did not reach the target angle. In the experiment conducted at this time, to make it easy to ascertain the difference between the angle limitation and the nonlimitation time, the target angle under position control was set as -45° to $+20^\circ$, restricted at the 0° position. Additionally, it was set to operate 1 s after the start of measurement. Figure 8 presents the results of control experiments with and without angle limits.

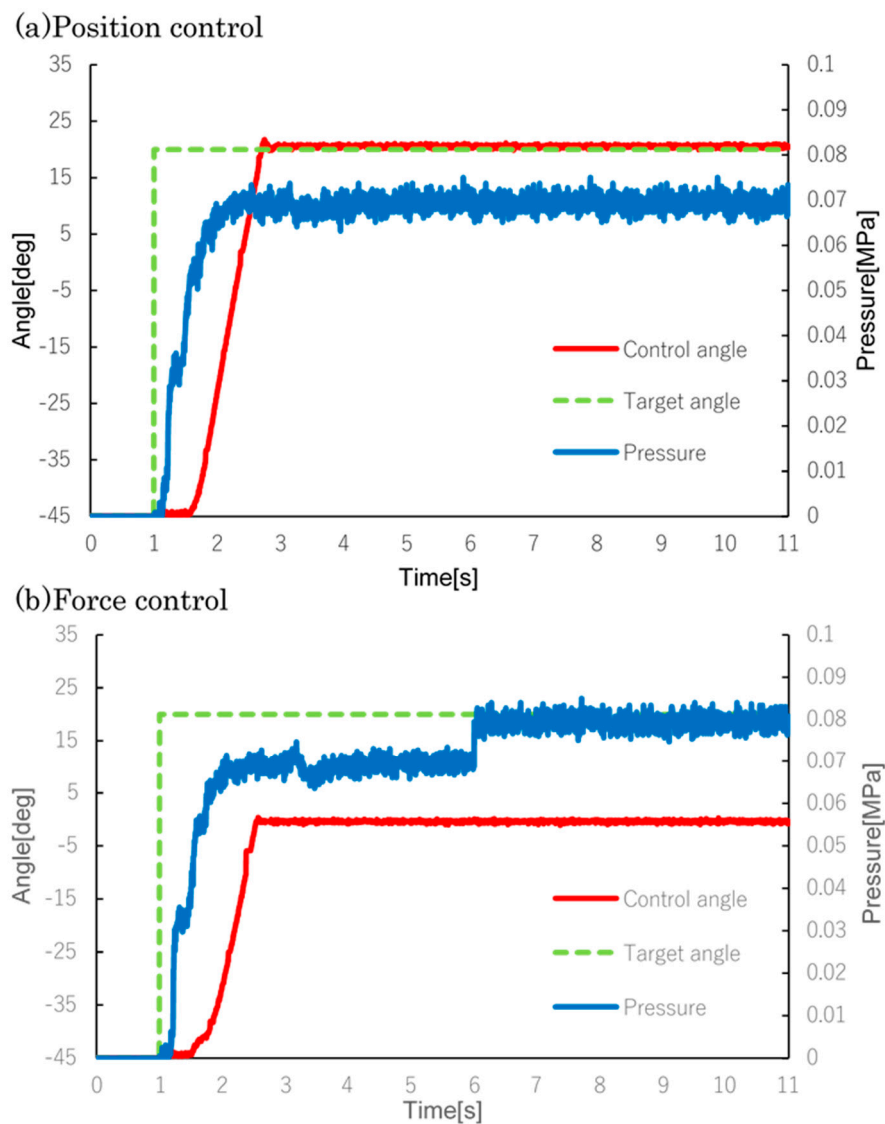


Figure 8. Switching control results when the angle is unrestricted. Left axis shows rotation angle, right axis shows applied pressure, horizontal axis shows time. Since the target angle is reached by 6 s, the applied pressure does not change.

Figure 8a shows that when the target angle is reached, it can be confirmed that the position control continues as it is. As presented in Figure 8b, even if the position control is performed by angle restriction, the target angle cannot be reached within 6 s; after 6 s, the air pressure under position control increases. It is understood that position control is switched to force control. In actual measurement results, applied pressure for 1–6 s at the time of angle restriction was 0.072 MPa and the foot reaction force was 29.6 N in the calculated value. The applied pressure after 6 s increased to 0.08 MPa and the

calculated foot reaction force reached 32.9 N. Results demonstrate that the force applied to the sole increased by 10% by switching to force control.

4. Ankle Neurorehabilitation System (ANS)

4.1. System Setup

Figure 9 shows the ankle neurorehabilitation system. This system consists of three subsystems: EEG measurement system, heuristic BCI system of learning fuzzy template matching (L-FTM), and the ARD. First, the EEG signals were detected, then they were signal-processed and passed to the L-FTM algorithm. The motor intention was extracted by the algorithm output signals, which were passed to the actual ARD, where the rehabilitation training was conducted.

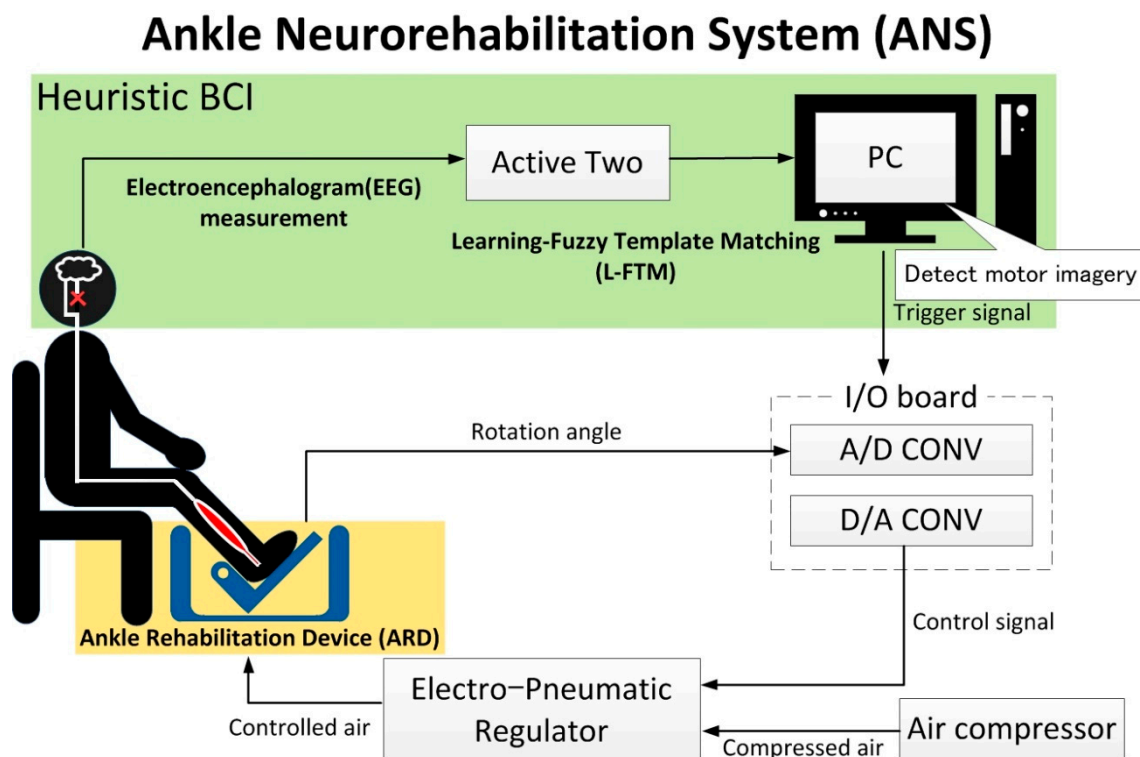


Figure 9. Ankle neurorehabilitation system, showing the experimental setup and signal transfer path.

The task was to use motor imagery of the right ankle at 30°. EEG signals produced during the task and a resting period were detected. The EEG signals were sent to the amplifier, where A/D conversion was done, then through a USB receiver (via optical fiber) to a PC for data processing. The sampling frequency was 2048 Hz. Then, in the learning process of the heuristic BCI, the values found using MATLAB 2018 software (Mathworks Inc., Natick, MA, USA) were applied to elucidate the task and nontask status. Here, the learning coefficient was set to 0.9, and the teacher signal was set to five in the task condition and 0 in the nontask condition. When the heuristic BCI-processed EEG signal surpassed the threshold, a triggering signal was generated and sent to a data acquisition device (USB-6000, National Instruments Corp., Austin, TX, USA). It was also sent by the trigger sending device (sampling frequency 2048 Hz; MARQ, Kissei Comtec Co. Ltd., Matsumoto, Japan) to the trigger receiver. This receiver was connected to another PC, where LabVIEW 2015 software processes controlled the triggering signals. Here, the triggering signal sent commands to where the rehabilitation device operates the pull up by 30° for a duration of 20 s. The thresholds, set by direct visualization, were initially set lower to detect motor imagery signals, but were later refined to exclude weaker L-FTM signals of resting EEG. The rehabilitation device is activated by air pressure generated

by a compressed air supply through a compressor (YC-4, Yaezaki-Kuatsu Co., Ltd., Tokyo, Japan) to the electropneumatic regulator (RTR-200-1, Koganei Corp., Tokyo, Japan). Control signals are sent through an I/O board (MF634, Humusoft Ltd., Praha, Czech). The rotation angle is measured using a potentiometer (SVO1, Murata Manufacturing Co. Ltd., Kyoto, Japan). Data from the potentiometer are sent through the I/O board to the PC.

4.2. Experimental Procedure

Five volunteers (22–24 years old, all healthy male students) participated in the experiment. The experiment followed the Kwansai Gakuin University regulations of ethics for the Protection of Human Subjects of Medical Research, which was approved by the campus committee. Informed consent was obtained from each participant. The study protocol conforms to the Declaration of Helsinki. Each participant was seated on a chair in a relaxed position with the right leg on the footrest with the ankle bent in a natural position. The left leg remained on the floor. EEG signals were detected using the Active Two system with eight electrodes (F3, F4, C3, Cz, C4, P3, Pz, and P4) based on the conventional 10–20 method. Only alpha (8–12 Hz) and beta (13–50 Hz) bandwidths were used for the heuristic BCI using L-FTM detection.

4.3. Experimental Protocol

Using the system explained above, we first verified that the signal of motor imagery of ankle uplift movement was indeed detected, which in turn operated the machinery. The experiment was conducted in three stages: (1) develop and practice motor imagery for the participant, (2) tune up the system to determine the parameters of motor imagery EEG, and (3) test motor imagery EEG to use the device to activate machinery.

For motor imagery development, voluntary upward movement of the right ankle was done first (voluntary task: 30 trials). (I) Motor imagery of the voluntary movement immediately followed (imagery task: 30 trials). The machine produced autonomous ankle movements simulating human rehabilitation behavior (autonomous movement task: 30 trials). Each trial was initiated by a trigger LED and each consisted of 4 s periods. EEG was done during this session. (II) The second process of system tune-up consisted of two substeps during which (a) EEG signals of the motor imagery were detected (2 min) (for comparison, a baseline EEG signal was measured during the resting period (2 min)), and (b) the heuristic BCI system using the L-FTM algorithm was applied to ascertain parameters to discriminate the two states of motor imagery and resting EEG. The FTM calculation took 60 s. (III) Finally, as the third step, the heuristic BCI system using L-FTM logic was tested by detecting the real motor imagery EEG. A trigger signal was generated as the output FTM signal. As soon as the system detected the motor imagery EEG, the triggering signal was presumed to be generated, which was to be transferred to the robot system. To verify this point, two tasks took place: participants were asked to (1) employ motor imagery when the LED light was illuminated, and (2) rest in order to test the resting EEG signal.

To analyze the brain activity tendency, independent component analysis was carried out using EEGLAB [20]. The EEG signal was first notch-filtered (60 ± 0.5 Hz and 120 ± 0.5 Hz bandwidth) to exclude artifacts from the electrical current, followed by band-pass filtering with frequencies of 0.04–200 Hz (finite impulse response (FIR) filtering). Special care was taken to minimize the notch filter artifacts when determining optimal bandwidth.

5. Results

Figure 10 shows the heuristic BCI outputs and the system thresholds, triggering position, and rotation angle. When the output value of the heuristic BCI surpassed the threshold, a trigger was generated and the rehabilitation device was operated. It is noteworthy that the system was programmed such that the rotation angle was kept constant for 20 s once the trigger was generated. Extra triggers during this period were ignored. After the 20 s period, another trigger can operate the system.

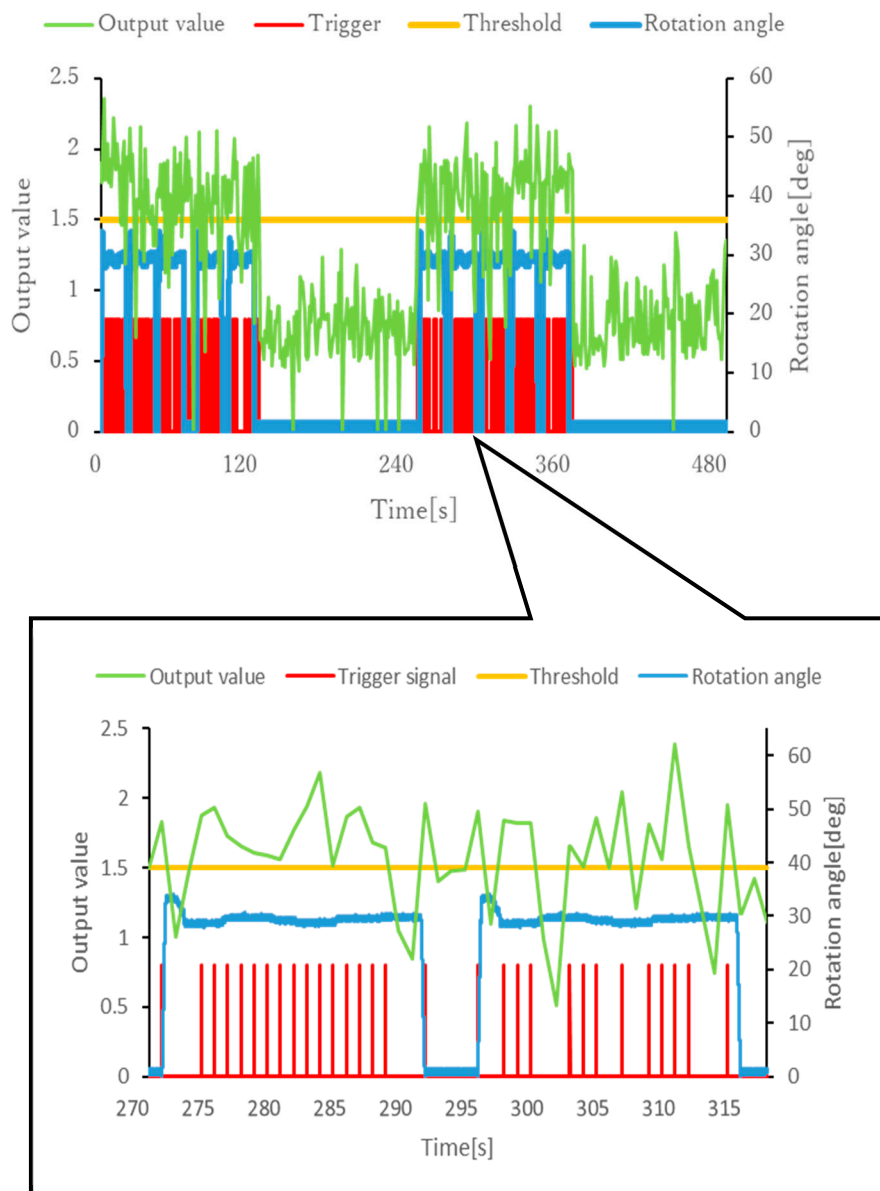


Figure 10. Heuristic BCI output and actual ankle rehabilitation device (ARD) performance.

The motor imagery effect on the EEG was compared with the control condition in which the machine moves the leg autonomously with the heuristic BCI algorithm [15,16]. Each column in Figure 10 shows independent component analysis (ICA) [21,22], where the relative activation area is highlighted in red as compared with a less activated area in blue and an average one in green. ICA results indicate that the overall EEG power was stronger during the test period, when the ankle rehabilitation system using heuristic BCI was used during motor imagery (Figure 11a) compared to the period with autonomous movement (Figure 11b). Results demonstrate that the activity around Cz was more conspicuous for movement with motor imagery. This result shows that the brain signals of the EEG increased with motor imagery, which was used to operate the rehabilitation system.

The additional average value of brain activity of the Cz channel is shown at rest, during voluntary movement, during passive movement, and during neurorehabilitation in the bar graph of Figure 12. Two-sided *t*-test for each task compared to rest showed a significant difference of more than 5% in all tasks.

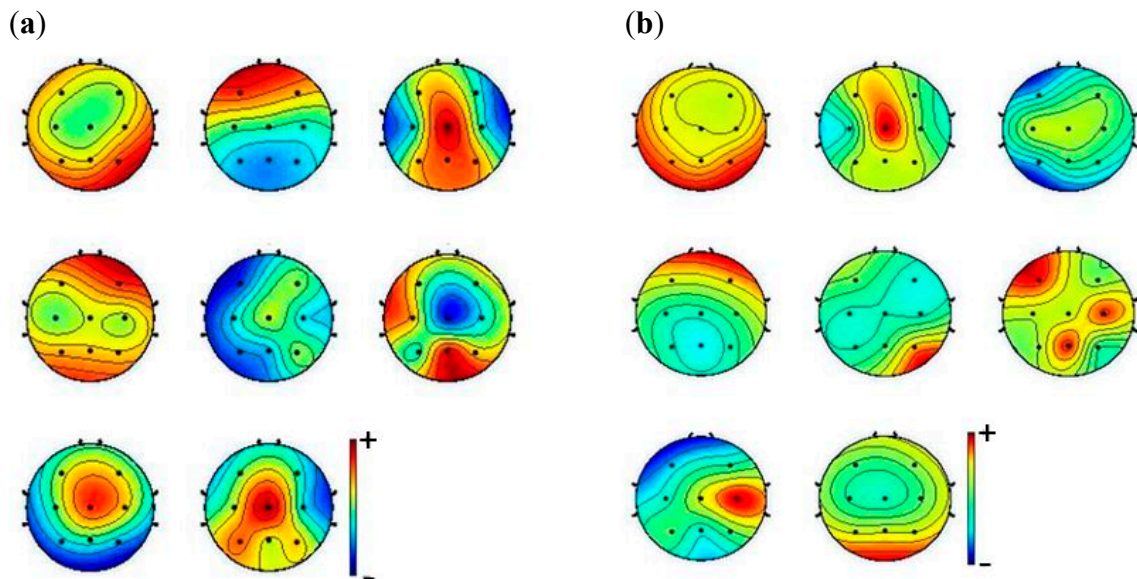


Figure 11. Results of independent component analysis (ICA) indicating that overall EEG power was stronger during the test period: (a) neurorehabilitation; (b) autonomous movement.

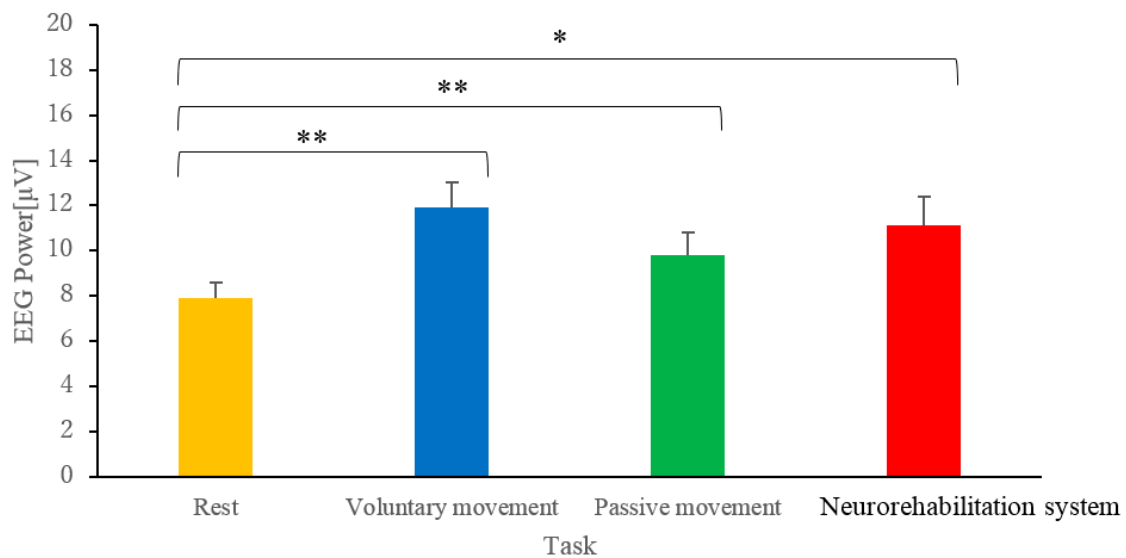


Figure 12. Additional average ICA results for each task. * $p < 0.05$, ** $p < 0.01$.

6. Conclusions

For this study, we developed an integrated neurorehabilitation system incorporating the human brain and a machine through a computer processing algorithm of the heuristic BCI using L-FTM. An important benefit of the system is that it allows detection of motor intention extremely quickly, within an hour, and requires no training of participants.

- The heuristic BCI was developed to identify EEG characteristics based on the motion intention (image) and to confirm that the trigger signal can be output. The most peculiar aspect of the heuristic BCI is its robustness in classifying the two states of EEG brain signals: the task state and the nontask state of brain activity. Its fuzzy characteristic is where the algorithm does not yield the perfect answer, but instead gives a rather crude (quick and dirty) answer within a short time. Here, frequencies of two kinds, alpha and beta bandwidths, were chosen, which markedly limits the inquiry search space, and therefore yielded a significantly short search time. An instant answer of 65,536 rules was obtained almost on time.

- Switching the control of position and force is realized automatically according to the patient's degree of joint contracture. This result shows that for patients with contracture, rehabilitation training can be performed on their own without the need for presetting by therapists.
- Using the system, activation of brain activity near the Cz channel was observed. The rehabilitation effect was observed. This result indicates that the motor area is activated, and it is considered that rehabilitation strongly connecting the motor intention and the rehabilitation motion is performed.

As the next stage of research, we will evaluate the effectiveness of this system by many brain-damaged patients undergoing rehabilitation. In addition, we will review the frequency band, measurement channels, etc., so that the heuristic BCI can be further optimized and shortened.

Author Contributions: N.S. wrote the paper and designed this system; Y.T. designed the system and analyzed the EEG data; A.D. performed the experiments and analyzed the experimental data; T.O. and S.N.K. designed the heuristic BCI system; H.F. performed the experiments.

Funding: This research was funded partially by the Ministry of Education, Culture, Sports, Science and Technology Supported Program for the Strategic Research Foundation at Private Universities, 2014–2018 (Grant No. S1411038) and Kansai Gakuin University.

Conflicts of Interest: The authors declare no conflict of interest.

References

1. Ministry of Internal Affairs and Communications statistics Bureau, population of the elderly, announced on 15 September 2016. Available online: <http://www.stat.go.jp/data/jinsui/pdf/201807.pdf> (accessed on 6 February 2018).
2. Ministry of Health, Labor and Welfare: Overview of the 2010 National Survey of Living in Japan. Available online: <http://www.mhlw.go.jp/toukei/saikin/hw/k-tyosa/k-tyosa10/4-2.html> (accessed on 6 February 2018).
3. Kintec: Kintec Brevia Ankle CPM. Available online: <http://kinetecuk.com/treatment-areas/foot-ankle/continuous-passive-motion/kinetec-brevia> (accessed on 13 February 2018).
4. Michmizos, K.P.; Rossi, S.; Castelli, E.; Cappa, P.; Krebs, H.I. Robot-aided neurorehabilitation: A pediatric robot for ankle rehabilitation. *IEEE Trans. Neural Syst. Rehabil. Eng.* **2015**, *23*, 1056–1067. [[CrossRef](#)] [[PubMed](#)]
5. Mattout, J.; Perrin, M.; Bertrand, O.; Maby, E. Improving BCI performance through co-adaptation: Applications to the P300-speller. *Ann. Phys. Rehabil. Med.* **2015**, *58*, 23–28. [[CrossRef](#)] [[PubMed](#)]
6. Liu, Y.; Higuchi, S.; Motohashi, Y. Time-of day effects of ethanol consumption on EEG topography and cognitive event-related potential in adult males. *J. Phys. Anthropol. Appl. Hum. Sci.* **2000**, *19*, 249–254. [[CrossRef](#)]
7. McDaid, A.J.; Xing, S.; Xie, S.Q. Brain Controlled Robotic Exoskeleton for Neurorehabilitation. In Proceedings of the 2013 IEEE/ASME International Conference on Advanced Intelligent Mechatronics, Wollongong, NSW, Australia, 9–12 July 2013; pp. 1039–1044.
8. Norcia, A.M.; Appelbaum, L.G.; Ales, J.M.; Cottreau, B.R.; Rossin, B. The steady-state visual evoked potential in vision research: A review. *J. Vis.* **2015**, *15*, 1–46. [[CrossRef](#)] [[PubMed](#)]
9. Kawahira, K.; Shimodozono, M.; Ogata, S.; Tanaka, N. Addition of intensive repetition of facilitation exercise to multidisciplinary rehabilitation promotes motor functional recovery of the hemiplegic lower limb. *J. Rehabil. Med.* **2004**, *36*, 159–164. [[CrossRef](#)] [[PubMed](#)]
10. Kwahira, K.; Noma, T.; Iiyama, J.; Etoh, S.; Ogata, A.; Shimodozono, M. Improvements in limb kinetic apraxia by repetition of a newly designed facilitation exercise in a patient with corticobasal degeneration. *Int. J. Rehabil. Res.* **2009**, *32*, 178–183. [[CrossRef](#)] [[PubMed](#)]
11. Frolov, A.A.; Mokienko, O.; Lyukmanov, R.; Biryukova, E.; Kotov, S.; Turbina, L.; Nadareyshvily, G.; Bushkova, Y. Post-stroke Rehabilitation Training with a Motor-Imagery-Based Brain-Computer Interface (BCI)-Controlled Hand Exoskeleton: A Randomized Controlled Multicenter Trial. *Front. Neurosci.* **2017**, *11*, 1–11. [[CrossRef](#)] [[PubMed](#)]
12. Takagi, T.; Sugeno, M. Fuzzy identification of systems and its applications to modeling and control. *IEEE Trans. Syst. Man Cybern.* **1985**, *15*, 116–132. [[CrossRef](#)]

13. Yachida, M.; Wu, H.; Chen, Q. Face Detection from Color Images Using a Fuzzy Pattern Matching Method. *IEEE Trans. PAMI* **1999**, *21*, 557–563.
14. Li, Y.; Qi, X.; Wang, Y. Eye Detection by using Fuzzy Template Matching and Feature Parameter Based Judgement. *Pattern Recognit. Lett.* **2001**, *22*, 1111–1124. [[CrossRef](#)]
15. Kudoh, S.N.; Tokuda, M.; Kiyohara, A.; Hosokawa, C.; Taguchi, T.; Hayashi, I. Vitroid-the robot system with an interface between a living neuronal network and outer world. *Int. J. Mechatron. Manuf. Syst.* **2011**, *4*, 135–149. [[CrossRef](#)]
16. Oda, T.; Kudoh, S.N. Identification of multiple-tasks-induced-EEG by heuristic BCI with learning type fuzzy-template-matching method. In Proceedings of the 2017 Joint 17th World Congress of International Fuzzy Systems Association and 9th International Conference on Soft Computing and Intelligent Systems (IFSA-SCIS), Otsu, Japan, 27–30 June 2017. [[CrossRef](#)]
17. Saga, N.; Saito, N. Rehabilitation instrument for prevent contracture of ankle using the pneumatic balloon actuator. In Proceedings of the 30th Annual International Conference of the IEEE Engineering in Medicine and Biology Society, Saga, Japan, 1 January 2008; pp. 4294–4297.
18. Saga, N.; Saito, N.; Nagase, J. Ankle Rehabilitation Device to Prevent Contracture Using a Pneumatic Balloon Actuator. *Int. J. Autom. Technol.* **2011**, *5*, 538–543. [[CrossRef](#)]
19. Japanese Body Size Data Book. Research Institute of Human Engineering for Quality Life. Available online: https://www.hql.jp/database/cat/etc/nite_h13-14_funcdb (accessed on 1 April 2019).
20. Delorme, A.; Makeig, S. EEGLAB: An open source toolbox for analysis of signal-trial EEG dynamics including independent component analysis. *J. Neurosci. Methods* **2004**, *134*, 9–21. [[CrossRef](#)] [[PubMed](#)]
21. Hyvarinen, A.; Oja, E. Independent component analysis: Algorithms and applications. *Neural Netw.* **2000**, *13*, 411–430. [[CrossRef](#)]
22. Bell, A.J.; Sejnowski, T.J. An information-maximization approach to blind separation and blind deconvolution. *Neural Comput.* **1995**, *7*, 1129–1159. [[CrossRef](#)] [[PubMed](#)]



© 2019 by the authors. Licensee MDPI, Basel, Switzerland. This article is an open access article distributed under the terms and conditions of the Creative Commons Attribution (CC BY) license (<http://creativecommons.org/licenses/by/4.0/>).